IOP Conf. Series: Materials Science and Engineering **199** (2017) 012087 doi:10.1088/1757-899X/199/1/012087

A Case Study of Wind-PV-Thermal-Bundled AC/DC Power Transmission from a Weak AC Network

H W Xiao[1], W J DU[1], H F WANG[1], Y T SONG[2], Q WANG[2], J DING[2], D Z CHEN[2] and W Wei[3]

[1]State Key Laboratory of Alternate Electrical Power System With Renewable Energy Sources. North China Electric Power University, Beijing, China
[2]China Electric Power Research Institute, Beijing, China
[3]Sichuan Electric Power Research Institute, Sichuan, china

Email: 530089657@qq.com

Abstract. Wind power generation and photovoltaic (PV) power generation bundled with the support by conventional thermal generation enables the generation controllable and more suitable for being sent over to remote load centre which are beneficial for the stability of weak sending end systems. Meanwhile, HVDC for long-distance power transmission is of many significant technique advantages. Hence the effects of wind-PV-thermal-bundled power transmission by AC/DC on power system have become an actively pursued research subject recently. Firstly, this paper introduces the technical merits and difficulties of wind-photovoltaic-thermal bundled power transmission by AC/DC systems in terms of meeting the requirement of large-scale renewable power transmission. Secondly, a system model which contains a weak wind-PV-thermal-bundled sending end system and a receiving end system in together with a parallel AC/DC interconnection transmission system is established. Finally, the significant impacts of several factors which includes the power transmission ratio between the DC and AC line, the distance between the sending end system and receiving end system, the penetration rate of wind power and the sending end system structure on system stability are studied.

1. Introduction

With the increasingly serious energy crisis, the development of renewable energy is being paid more and more attention. At present, although the fossil energies such as coal, oil and natural gas are still in the dominant position, but due to the fossil energy holds the disadvantages of limit in storage capacity and the undesirable impacts on the environment, all countries begin to seek for alternative renewable energy actively. So in the past decades, wind power generation technology and photovoltaic (PV) power generation technology have been developed rapidly. However, with the proportion of renewable energy power integration increasing, the effect on the stability of power system is deteriorating, especially in a weak AC system that contains wind power, PV power and DC line. The interactions of wind power, PV power and DC line are complex, and the effect on the stability of power system needs further research.

Currently, there are few researches on the wind-PV-thermal-bundled transmitted by AC/DC system, and the interactions between the renewable energy power and the DC line have not been determined. There are several factors that may have great influences on power system stability based on the previous researches [1]-[5]. In this paper, we mainly study the influences of the five factors on the stability of the system, which contains the penetration rate of wind power, the distance between the sending end system and the receiving end system, the capacity of power that transmitted through the DC line, and the structure of the sending end system.

2. Wind-PV-Thermal-Bundled transmitted by AC/DC from a weak system

In order to find out the factors what may have great influences on power system stability, we set up a simulation system showing in Fig. 1 in the PSASP.

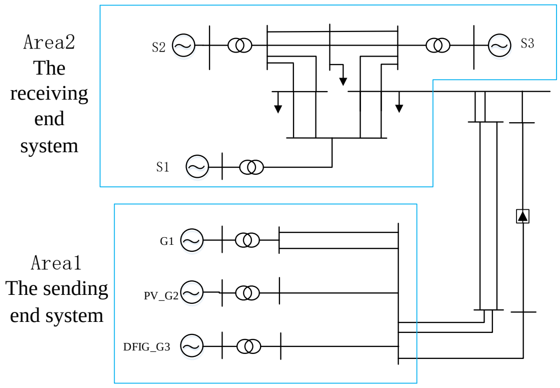

Figure 1. The wind-PV-thermal-bundled transmitted by AC/DC system.

In the Fig. 1, the wind-PV-thermal-bundled power source is Y-connected in the Area1, and the capacity of the three power sources is 600MW, 200MW and 1000MW respectively. Meanwhile, the receiving end system isΔ-connected in Area 2, and the distance between the generations in the receiving end system is shorter than that in the sending end system. By the above settings, we construct a weak sending end system and a strong receiving end system. In this system, we mainly study the influences of the five factors on the small-signal stability of the 2.1.

3. The small disturbance stability of the system

It is difficult to avoid the occurrence of the small-signal during the power system operation, so small-signal stability is the premise of normal operation of the power system, which means the small-signal stability analysis is important for the stable operation of the power system. We need to linear the dynamic element equation of the power system before the small-signal stability analysis. In the system showing in Fig. 1, the dynamics what need to be considered are synchronous machine, DFIG, PV and DC line. [6]-[8]

The formation of the linear differential equations of the whole system showing in Fig. 1

Network equation of the whole system:

$$\begin{bmatrix} \Delta\mathbf{I}_G \\ \Delta\mathbf{I}_W \\ \Delta\mathbf{I}_P \\ \Delta\mathbf{I}_D \\ \mathbf{0} \end{bmatrix} = \begin{bmatrix} \mathbf{Y}_{GG} & \mathbf{Y}_{GW} & \mathbf{Y}_{GP} & \mathbf{Y}_{GD} & \mathbf{Y}_{GL} \\ \mathbf{Y}_{WG} & \mathbf{Y}_{WW} & \mathbf{Y}_{WP} & \mathbf{Y}_{WD} & \mathbf{Y}_{WL} \\ \mathbf{Y}_{PG} & \mathbf{Y}_{PW} & \mathbf{Y}_{PP} & \mathbf{Y}_{PD} & \mathbf{Y}_{PL} \\ \mathbf{Y}_{DG} & \mathbf{Y}_{DW} & \mathbf{Y}_{DP} & \mathbf{Y}_{DD} & \mathbf{Y}_{DL} \\ \mathbf{Y}_{LG} & \mathbf{Y}_{LW} & \mathbf{Y}_{LP} & \mathbf{Y}_{LD} & \mathbf{Y}_{LL} \end{bmatrix} \begin{bmatrix} \Delta\mathbf{V}_G \\ \Delta\mathbf{V}_W \\ \Delta\mathbf{V}_P \\ \Delta\mathbf{V}_D \\ \Delta\mathbf{V}_L \end{bmatrix} \tag{1}$$

Where, $\Delta\boldsymbol{I}_G = [\Delta I_{S1} \quad \Delta I_{S2} \quad \Delta I_{S3} \quad \Delta I_{G1}]^T$, $\Delta\boldsymbol{I}_P = [\Delta I_{p1}]^T$, $\Delta\boldsymbol{I}_W = [\Delta I_{W1}]^T$, $\Delta\boldsymbol{I}_D = [\Delta I_{D1}]^T$, $\Delta\boldsymbol{V}_G = [\Delta V_{S1} \quad \Delta V_{S2} \quad \Delta V_{S3} \quad \Delta V_{G1}]^T$, $\Delta\boldsymbol{V}_P = [\Delta V_{P1}]^T$, $\Delta\boldsymbol{V}_W = [\Delta V_{W1}]^T$, $\Delta\boldsymbol{V}_D = [\Delta V_{D1}]^T$.

The linear differential equation of the synchronous machine:

$$\begin{aligned} \frac{d\Delta \mathbf{x}_G}{dt} &= \mathbf{A}_G \Delta \mathbf{x}_G + \mathbf{B}_G \Delta \mathbf{V}_G \\ \Delta \mathbf{I}_G &= \mathbf{C}_G \Delta \mathbf{x}_G + \mathbf{D}_G \Delta \mathbf{V}_G \end{aligned} \tag{2}$$

The linear differential equation of the DFIG:

$$\begin{aligned} \frac{d\Delta \mathbf{x}_W}{dt} &= \mathbf{A}_W \Delta \mathbf{x}_W + \mathbf{B}_W \Delta \mathbf{V}_W \\ \Delta \mathbf{I}_W &= \mathbf{C}_W \Delta \mathbf{x}_W + \mathbf{D}_W \Delta \mathbf{V}_W \end{aligned} \tag{3}$$

The linear differential equation of the PV:

$$\begin{aligned} \frac{d\Delta \mathbf{x}_P}{dt} &= \mathbf{A}_P \Delta \mathbf{x}_P + \mathbf{B}_P \Delta \mathbf{V}_P \\ \Delta \mathbf{I}_P &= \mathbf{C}_P \Delta \mathbf{x}_P + \mathbf{D}_P \Delta \mathbf{V}_P \end{aligned} \tag{4}$$

The linear differential equation of the DC line:

$$\begin{aligned} \frac{d\Delta \mathbf{x}_D}{dt} &= \mathbf{A}_D \Delta \mathbf{x}_D + \mathbf{B}_D \Delta \mathbf{V}_D \\ \Delta \mathbf{I}_D &= \mathbf{C}_D \Delta \mathbf{x}_D + \mathbf{D}_D \Delta \mathbf{V}_D \end{aligned} \tag{5}$$

From (1) (2) (3) (4) (5), there is equivalently expressed as:

$$\begin{bmatrix} \frac{d\Delta \mathbf{x}}{dt} \\ 0 \end{bmatrix} = \begin{bmatrix} \mathbf{A} & \mathbf{B} \\ \mathbf{C} & \mathbf{D} \end{bmatrix} \begin{bmatrix} \Delta \mathbf{x} \\ \Delta \mathbf{y} \end{bmatrix} \tag{6}$$

Where

$$\mathbf{A} = \begin{bmatrix} \mathbf{A}_G & 0 & 0 & 0 \\ 0 & \mathbf{A}_W & 0 & 0 \\ 0 & 0 & \mathbf{A}_T & 0 \\ 0 & 0 & 0 & \mathbf{A}_D \end{bmatrix}, \mathbf{B} = \begin{bmatrix} \mathbf{B}_G & 0 & 0 & 0 & 0 \\ 0 & \mathbf{B}_W & 0 & 0 & 0 \\ 0 & 0 & \mathbf{B}_P & 0 & 0 \\ 0 & 0 & 0 & \mathbf{B}_D & 0 \end{bmatrix} \mathbf{C} = \begin{bmatrix} -\mathbf{C}_G & 0 & 0 & 0 \\ 0 & -\mathbf{C}_W & 0 & 0 \\ 0 & 0 & -\mathbf{C}_P & 0 \\ 0 & 0 & 0 & -\mathbf{C}_D \\ 0 & 0 & 0 & 0 \end{bmatrix}$$

$$\mathbf{D} = \begin{bmatrix} \mathbf{Y}_{GG} - \mathbf{D}_G & \mathbf{Y}_{GW} & \mathbf{Y}_{GP} & \mathbf{Y}_{GD} & \mathbf{Y}_{GL} \\ \mathbf{Y}_{WG} & \mathbf{Y}_{WW} - \mathbf{D}_W & \mathbf{Y}_{WP} & \mathbf{Y}_{WD} & \mathbf{Y}_{WL} \\ \mathbf{Y}_{PG} & \mathbf{Y}_{PW} & \mathbf{Y}_{PP} - \mathbf{D}_P & \mathbf{Y}_{PD} & \mathbf{Y}_{PL} \\ \mathbf{Y}_{DG} & \mathbf{Y}_{DW} & \mathbf{Y}_{DP} & \mathbf{Y}_{DD} - \mathbf{D}_D & \mathbf{Y}_{DL} \\ \mathbf{Y}_{LG} & \mathbf{Y}_{LS} & \mathbf{Y}_{LT} & \mathbf{Y}_{LD} & \mathbf{Y}_{LL} \end{bmatrix}$$

$\Delta \mathbf{x} = \left[\Delta \mathbf{x}_G \quad \Delta \mathbf{x}_W \quad \Delta \mathbf{x}_P \quad \Delta \mathbf{x}_D \right], \Delta \mathbf{y} = \left[\Delta \mathbf{V}_G \quad \Delta \mathbf{V}_W \quad \Delta \mathbf{V}_P \quad \Delta \mathbf{V}_D \quad \Delta \mathbf{V}_L \right]$

In the equation (6), after eliminating the vector $\Delta \mathbf{y}$, it can be shown that:

$$\frac{d\Delta \mathbf{x}}{dt} = \mathbf{A}_r \Delta \mathbf{x} \tag{7}$$

Where $\mathbf{A}_r = \mathbf{A} - \mathbf{B}\mathbf{D}^{-1}\mathbf{C}$.

Whether the system is stable can be determined through calculation eigenvalue of the state matrix $\mathbf{A}_r$.

4. Factors that influence the small-signal stability of the system

4.1. The influence of the distance between the generator of the sending end system on the small-signal stability of the system.

In order to study the influence of the distance between the generators of the sending end system on the small-signal stability of the system, small-signal stability analysis has been done under different situations, the results are shown in Table 1:

Table 1. The results of small-signal stability analysis

The distance between the generator of the sending end system is 50 Km					
	Eigenvalue	Frequency (Hz)	Damping ratio (%)	Most relevant generator	Region
1	-0.785±7.237i	1.152	10.783	S2	Area2
2	-0.687±5.732i	0.912	11.894	S3	Area2
3	-0.409±4.615i	0.735	8.830	G1	Area1
The distance between the generator of the sending end system is 70 Km					
	Eigenvalue	Frequency (Hz)	Damping ratio (%)	Most relevant generator	Region
1	-0.785±7.263i	1.156	10.747	S2	Area2
2	-0.722±5.689i	0.905	12.586	S3	Area2
3	-0.351±4.376i	0.696	8.000	G1	Area1
The distance between the generator of the sending end system is 90 Km					
	Eigenvalue	Frequency (Hz)	Damping ratio (%)	Most relevant generator	Region
1	-0.785±7.282i	1.159	10.720	S2	Area2
2	-0.735±5.678i	0.904	12.832	S3	Area2
3	-0.319±4.240i	0.675	7.505	G1	Area1

Comparing the small-signal stability analysis results of the three situations, it can be found that the eigenvalues related to G1 moves to the right when the distance between the generator of the sending end system is increased, which means the small-signal stability of the sending end system is worsen.

4.2. The influence of the penetration rate of wind power on the small-signal stability of the system

In order to study the influence of the penetration rate of wind power on the small-signal stability of the system, thermal power is replaced by equal capacity of wind power, which can change the penetration rate of wind power. By this method, the small-signal stability analysis has been done under three different situations, the results are shown in Table 2:

Table 2. The results of small-signal stability analysis

Thermal power 1000MW, Wind power 600MW, PV power 200MW					
	Eigenvalue	Frequency (Hz)	Damping ratio (%)	Most relevant units	Region
1	-0.785±7.237i	1.152	10.783	S2	Area2
2	-0.687±5.732i	0.912	11.894	S3	Area2
3	-0.409±4.615i	0.735	8.830	G1	Area1
Thermal power 800MW, Wind power 800MW, PV power 200MW					
	Eigenvalue	Frequency (Hz)	Damping ratio (%)	Most relevant units	Region
1	-0.785±7.239i	1.152	10.780	S2	Area2
2	-0.707±5.723i	0.911	12.258	S3	Area2

3	-0.433±4.552i	0.724	9.471	G1	Area1
Thermal power 600MW, Wind power 1000MW, PV power 200MW					
	Eigenvalue	Frequency (Hz)	Damping ratio (%)	Most relevant units	Region
1	-0.785±7.250	1.154	10.768	S2	Area2
2	-0.737±5.698	0.907	12.822	S3	Area2
3	-0.461±4.371	0.696	10.479	G1	Area1

Comparing the results of the small-signal stability analysis under the three situations, it can be found that when the penetration rate of wind power increases, the eigenvalues related to G1 move to the left which means the small-signal stability is improved.

4.3. The influence of the distance between the sending end system and the receiving end system on the small-signal stability of the system.

The length of the AC/DC line can denote the distance between the sending end system and the receiving end system. In order to study the influence of the distance between the sending end system and the receiving end system on the small-signal stability of the system, small-signal stability analysis has been done under three different situations, the results are shown in Table 3:

Table 3. The results of small-signal stability analysis

The length of the AC/DC line is 1000Km					
	Eigenvalue	Frequency (Hz)	Damping ratio (%)	Most relevant units	Region
1	-0.785+7.237i	1.151	10.782	S2	Area2
2	-0.687+5.733i	0.912	11.894	S3	Area2
3	-0.409+4.615i	0.735	8.830	G1	Area1
The length of the AC/DC line is 1250Km					
	Eigenvalue	Frequency (Hz)	Damping ratio (%)	Most relevant units	Region
1	-0.785+7.251i	1.154	10.766	S2	Area2
2	-0.730+5.651i	0.899	12.808	S3	Area2
3	-0.332+4.268i	0.679	7.759	G1	Area1
The length of the AC/DC line is 1500Km					
	Eigenvalue	Frequency (Hz)	Damping ratio (%)	Most relevant units	Region
1	-0.785+7.265i	1.156	10.748	S2	Area2
2	-0.750+5.610i	0.893	13.245	S3	Area2
3	-0.282+3.926i	0.625	7.173	G1	Area1

Comparing the results of the small-signal stability analysis under the three situations, it can be found that increasing the distance between the sending end system and the receiving end system would lead to the eigenvalues related to G1 move to the right which means the small-signal stability is deteriorated.

4.4. The influence of the ratio of the power transmitted in AC/DC line on the small-signal stability of the system.

Because of the characteristic of the DC line, the power transmitted in the DC line can be adjusted according to our needs [9]. In order to study the influence of the ratio of the power transmitted in AC/DC line on the small-signal stability of the system, power transmitted in DC line is adjusted under the premise of the total transmission power remaining constant. By this method, the small-signal stability analysis has been done under three different situations, the results are shown in Table 4:

Table 4. The results of small-signal stability analysis

The ratio of the power transmitted in AC/DC is 1：1					
	Eigenvalue	Frequency (Hz)	Damping ratio (%)	Most relevant units	Region
1	-0.785+7.236i	1.152	10.784	S2	Area2
2	-0.693+5.718i	0.910	12.028	S3	Area2
3	-0.400+4.577i	0.729	8.713	G1	Area1
The ratio of the power transmitted in AC/DC is 1：2					
	Eigenvalue	Frequency (Hz)	Damping ratio (%)	Most relevant units	Region
1	-0.785+7.239i	1.152	10.782	S2	Area2
2	-0.668+5.773i	0.919	11.492	S3	Area2
3	-0.439+4.712i	0.750	9.273	G1	Area1
The ratio of the power transmitted in AC/DC is 1：3					
	Eigenvalue	Frequency (Hz)	Damping ratio (%)	Most relevant units	Region
1	-0.785+7.251i	1.154	10.766	S2	Area2
2	-0.659+5.804i	0.924	11.275	S3	Area2
3	-0.457+4.757i	0.757	9.555	G1	Area1

Comparing the results of the small-signal stability analysis under the three situations, it can be found that increasing the power transmitted in DC line will lead to the eigenvalues related to G1 move to the left which means the small-signal stability is improved.

4.5. The influence of the structure of the sending end system on the small-signal stability of the system.

In this research, we assume that the geographical positions of the three kinds of generators in sending end system are fixed, which are respectively at the three vertices of an equilateral triangle whose side length is $25\sqrt{3}$Km. Under this assumption, the small-signal stability analysis has been done under two different situations, the results are shown in Table 5:

Table 5. The results of small-signal stability analysis

Y-connection, the DC bus is at the centre of the equilateral triangle					
	Eigenvalue	Frequency (Hz)	Damping ratio (%)	Most relevant units	Region
1	-0.785+7.230i	1.151	10.793	S2	Area2
2	-0.655+5.752i	0.915	11.311	S3	Area2
3	-0.411+4.726i	0.752	8.673	G1	Area1
Δ-connection，the DC bus is at the location of the thermal power generator					

	Eigenvalue	Frequency (Hz)	Damping ratio (%)	Most relevant units	Region
1	-0.784+7.219i	1.149	10.800	S2	Area2
2	-0.566+4.943i	0.787	11.367	S3	Area2
3	-0.601+5.954i	0.948	10.046	G1	Area1

Comparing the results of the small-signal stability analysis, it can be found that increasing the power transmitted in DC line will lead to the eigenvalues related to G1 move to the left which means the small-signal stability is improved.

5. Discussion and prospect

Because of the advantage of the wind-PV-thermal-bundled power transmission by AC/DC system, it provides new opportunity for the wind power integration and the power transmission. Currently, we have find out some factors that may have great influence on the small-signal stability of the system, but it need deeper study before this scheme applies in practical project.

Currently, most researches on the wind-PV-thermal-bundled power transmission by AC/DC system are conducted in the simple system, but the structure of the sending system and the ending system can significantly influence the stability of the system. Thus, when the structure of the system is complex, the stability of the whole system are needed to study.

Acknowledgements

The work is supported by state grid cooperation of China (program XT71-15-059).

References

[1] GUO Xiaojiang1, ZHAO Lili2, TANG Yi2, SHEN Hong3. Study on Angle Transient Stability for Wind-thermal-bundled Power Transmitted by AC/DC System [J]. Proceedings of the CSEE, 2013, 22:19-25+6
[2] Zhu Yi Ying. Simulation and Coordination Control on Large Scale Wind and Thermal Power Transmission by HVDC [D]. North China Electric Power University, 2014
[3] ZHANG Bu-han, CHEN Long, LI Huang, LI Xiao-ping, ZHOU You-bin, HUANG Yong, ZENG Jie, MAO Cheng-xiong. Improving the Stability of UHV AC Interconnected System by the DC Power Modulation [J]. High Vol tage Engineering, 2010, 01:116-121
[4] LI Shengfu1, 2, ZHANG Ailing1, LI Shaohua1. Study on transient stability control for wind-thermal-bundled power transmitted by AC/DC system [J]. Power System Protection and Control,2015,01:108-114
[5] Peterson H A, Reitan D K, Phadke A G. Parallel Operation of AC and DC Power Transmission [J]. IEEE Transactions on Power Apparatus & Systems, 1965, 84(1):15-19
[6] Yuanzhang, WANG, Lixin, et al. A review on analysis and control of small signal stability of power systems with large scale integration of wind power[C]// Power System Technology (POWERCON), 2010 International Conference on. IEEE, 2010:1 – 6
[7] Wang L, Lin Y H. Small-signal stability and transient analysis of an autonomous PV system[J]. IEEE/PES Transmission & Distribution Conference & Exposition, 2008:1-6
[8] Zhao F, Li N, Yin Z, et al. Small-signal modeling and stability analysis of DC microgrid with multiple type of loads[C]// International Conference on Power System Technology. IEEE, 2014:3309-3315
[9] Taylor C W, Lefebvre S. HVDC controls for system dynamic performance[J]. IEEE Transactions on Power Systems, 1991, 6(2):743-752